CHIN. PHYS. LETT. Vol. 38, No. 1 (2021) 017302

Layered Transition Metal Electride Hf_2Se with Coexisting Two-Dimensional Anionic *d*-Electrons and Hf–Hf Metallic Bonds

Xihui Wang(王西惠)[1†], Xiaole Qiu(邱潇乐)[2†], Chang Sun(孙畅)[1], Xinyu Cao(曹新宇)[1], Yujie Yuan(袁宇杰)[1], Kai Liu(刘凯)[2*], and Xiao Zhang(张晓)[1*]

[1]*State Key Laboratory of Information Photonics and Optical Communications & School of Science, Beijing University of Posts and Telecommunications, Beijing 100876, China*

[2]*Department of Physics and Beijing Key Laboratory of Opto-electronic Functional Materials & Micro-nano Devices, Renmin University of China, Beijing 100872, China*

(Received 20 October 2020; accepted 18 November 2020; published online 6 January 2021)

Electrides are unique materials, whose anionic electrons are confined to interstitial voids, and they have broad potential applications in various areas. In contrast to the majority of inorganic electrides, in which the anionic electrons primarily consist of *s*-electrons of metals, electrides with anionic *d*-electrons are very rare. Based on first-principles electronic structure calculations, we predict that the layered transition metal chalcogenide Hf_2Se is a novel electride candidate with anionic *d*-electrons. Our results indicate that the anionic electrons confined in the Hf_6 octahedra vacancy between [Hf_2Se] layers mainly come from the Hf-5*d* orbitals. In addition, the anionic electrons coexist with the Hf–Hf multiple-center metallic bonds located in the center of neighboring Hf_4 tetrahedra. The calculated work function (3.33 eV) for the (110) surface of Hf_2Se is slightly smaller than that of Hf_2S, which has recently been reported to exhibit good electrocatalytic performance. Our study of Hf_2Se will enrich the electride family, and promote further research into the physical properties and applications of electrides.

DOI: 10.1088/0256-307X/38/1/017302

Electrides are peculiar materials, where electrons play the role of anions. Anionic electrons in electrides mostly tend to occupy the crystallographic interstitial sites, not belonging to any particular atoms or covalent bonds. The anionic electrons in electrides are also distinct from the itinerant electrons in metals because their wave functions are usually confined in the cavities between cations. Since the discovery of organic electrides,[1,2] various inorganic electrides with improved thermal stability have also been synthesized. In particular, the first inorganic electride $[Ca_{24}Al_{28}O_{64}]^{4+}\cdot 4e^-$ ($C_{12}A_7$) with low work function has an important application in terms of promoting the catalytic efficiency of ammonia synthesis at ambient pressure and low temperature.[3,4] In addition, some inorganic materials behave like electrides under extreme conditions. For example, anionic electrons in Na and Na_2He under high pressure are localized at the interstitial sites.[5,6] Due to their unique structural, physical, and chemical properties, inorganic electrides have attracted intense attention, both in terms of fundamental science and potential areas of application.

According to the dimensionality of anionic electron distributions, inorganic electrides can be classified as zero-dimensional (0D),[7] one-dimensional (1D),[8] two-dimensional (2D),[9–11] and three-dimensional (3D) electrides.[12] Of these, 2D electrides exhibit some distinctive properties. For example, in 2D electride Ca_2N,[9] the anionic electrons are partially delocalized and confined between neighboring Ca–N layers, becoming a 2D electron gas with rather high carrier mobility and concentrations in comparison with 0D electrides. More interestingly, Ca_2N can be exfoliated into thermally and mechanically stable thin flakes, where the electron gas is present on the surface.[13,14] This type of 2D electron gas can be used as a solid-state dopant to tune the physical properties of van der Waals 2D materials, e.g., the structural transition of few-layer $MoTe_2$ or graphene.[15,16]

The anionic electrons in most of the electrides discovered to date originate mainly from the *s*-orbital electrons of metals, while *d*-orbital electrides are very scarce. In 2D electride Y_2C and YCl, the *d* electrons of Y form polar covalent bonds with C and Y–Y metallic bonds, respectively, rather than anionic electrons.[10,17] Recently, 1D electride Sr_3CrN_3 is reported to have exhibited a partially filled *d* shell of Cr^{4+}, but whether the anionic electrons come from the Cr^{4+} or Sr^{2+} is subject to debate, since the Sr atoms are in the 1D electron channel.[18] Research

Supported by the National Natural Science Foundation of China (Grant No. 11774424), the Fundamental Research Funds for the Central Universities (Grant No. 2017RC20), the Research Funds of Renmin University of China (Grant No. 20XNH064), the CAS Interdisciplinary Innovation Team, the Beijing Natural Science Foundation (Grant No. Z200005), and the Research Innovation Fund for College Students of Beijing University of Posts and Telecommunications.

†Xihui Wang and Xiaole Qiu contributed equally to this work.

*Corresponding authors. Email: kliu@ruc.edu.cn; zhangxiaobupt@bupt.edu.cn

© 2021 Chinese Physical Society and IOP Publishing Ltd

to discover new electrides with anionic d-electrons is therefore very much required.

In addition to the experimental exploration of electrides, high-throughput computational screening, based on first-principles calculations and certain material design principles, provides another critical approach to the discovery of novel electrides.[19–23] Many potential electrides have been predicted, some of which have been verified by experiments, such as Y_2C, Sr_3CrN_3, Sr_8P_5, and Sr_5P_3.[10,18,23] Recently, the predicted layered electride Hf_2S with 2D anionic electrons has been successfully synthesized.[24] Analysis shows that a self-passivation behavior leads to a strong oxidation resistance in water and acid solutions, facilitating a persistent reaction for electrocatalytic hydrogen evolution.[24] Based on the above considerations, in this work, we theoretically explore the electronic structures and physical properties of an isostructural material, Hf_2Se. It is found that Hf_2Se is a 2D electride with anionic d-orbitals and Hf–Hf metallic bonds.

The electronic structure calculations of Hf_2Se in this work were performed based on the density functional theory (DFT), as implemented via the Vienna *ab initio* simulation package (VASP).[25] The electron–ion interactions were described using the projector-augmented wave (PAW) method.[25] A generalized gradient approximation in the Perdew–Burke–Ernzerhof form (GGA-PBE) was adopted for the exchange-correlation functional.[26] The plane-wave basis-set cutoff was set to 450 eV. A $22 \times 22 \times 6$ k-point grid for Brillouin zone sampling was used to optimize the structure and obtain a self-consistent solution of the Kohn–Sham equation. Optimized atomic positions were obtained via the total energy and force minimization method, where the minimum force criterion was 0.001 eV/Å. To determine the work function ($\Phi_{\rm WF}$) of Hf_2Se, two slab models for the (001) (18 atoms) and (110) (90 atoms) surfaces were constructed, perpendicular to or parallel to the edge-sharing metal octahedral layer, respectively. For these slab models, the vacuum was set to 20 Å. The respective k-point grids were $15 \times 15 \times 1$ and $7 \times 7 \times 1$ for the (001) and (110) surfaces. The values of $\Phi_{\rm WF}$ were calculated by means of the equation $\Phi_{\rm WF} = e\Phi_{\rm vac} - E_{\rm F}$, where $\Phi_{\rm vac}$ is the electrostatic potential of the vacuum region, and e is the electron charge.[27]

Figure 1(a) shows the structure of Hf_2Se with the space group $P63/mmc$ (No. 194).[28] The basic unit is the [Hf_2Se] layer, where Se atoms are sandwiched between Hf atoms, forming an edge-shared [Hf_6Se] trigonal prismatic coordination slab. These Hf–Se layers stack along the c-axis with an ABAB sequence, restoring the inversion symmetry. The a- and c-axial lattice constants of Hf_2Se are 3.44 Å and 12.32 Å, respectively, which are larger than those of the isostructural compound Hf_2S ($a = 3.37$ Å and $c = 11.79$ Å)[28] owing to the larger ionic radius of Se^{2-} ions. It should be noted that Hf_2Se has an anti-2H-NbS_2 structure, where the sites of Nb and S atoms are occupied inversely by Se and Hf atoms in Hf_2Se. The Hf–Se distance ($d_{\rm Hf-Se}$) in the [Hf_2Se] layer is 2.51 Å, comparable with that of 1T-$HfSe_2$ ($d_{\rm Hf-Se} = 2.65$ Å),[29] suggesting that the bonding between Hf and Se atoms in the [Hf_2Se] layer is primarily ionic. For most reported electrides, the formation of the interstitial void in the metal polyhedron is the key structural ingredient in the hosting of anionic electrons, such as the interlayer Ca_6 octahedra in Ca_2N and Y_6 octahedra in Y_2C.[9,10] Similarly, for Hf_2Se, two kinds of interstitial voids, comprising Hf_4 tetrahedra and Hf_6 octahedra, exist in the interlayer space. The interlayer distance $d_{\rm inter}$ in Hf_2Se is about 3.08 Å, similar to the thickness of the [Hf_2Se] layer. Compared with Ca_2N ($d_{\rm inter} = 3.86$ Å) and Y_2C ($d_{\rm inter} = 3.29$ Å),[9,10] the smaller interlayer distance in Hf_2Se implies that there may be more electrons between the [Hf_2Se] layers, leading to interlayer electrostatic interaction. Moreover, since the most stable valence state of Se ions is −2, and the valence state of Hf ion is usually +4, the [Hf_2Se] layer should be positively charged. Based on the requirements of charge neutrality, there are 6 excess electrons per Hf_2Se formula, indicating the intrinsic electron-rich character of Hf_2Se. These electrons locate at the interstitial sites between the [Hf_2Se] layers, which is consistent with the above analysis.

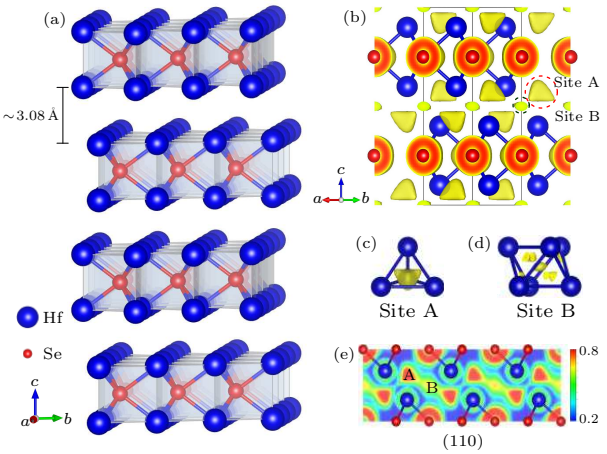

Fig. 1. (a) Crystalline structure of Hf_2Se with a hexagonal unit cell. (b) Calculated electron localization function (ELF) of Hf_2Se with an isosurface value of 0.65. The ELF attractors at the centers of the Hf_4 tetrahedron (site A) and Hf_6 octahedron (site B) are indicated by dashed red and blue circles, respectively. Enlarged views of the ELF attractors located at (c) site A and (d) site B. (e) The 2D ELF contour in the (110) plane.

In order to unveil the electride features of Hf_2Se, we have calculated the electron localization function (ELF) of Hf_2Se, which is widely used as an indicator of confined interstitial electrons in the electrides.[30,31] Figures 1(b)–1(e) depict the ELF results for Hf_2Se. The virtually spherically distributed ELF attractors around the cores of the Se atoms clearly indicate the

ionic bonding between Hf and Se atoms.[32] More importantly, there are two ELF attractors, located at the centers of the Hf_4 tetrahedron (site A, highlighted by the red circle) and the Hf_6 octahedron (site B, highlighted by the blue circle), between adjacent [Hf_2Se] layers. As shown in Figs. 1(c) and 1(d), the former is larger than the latter, and has a higher ELF value [Figs. 1(e)] when approaching the center of the tetrahedron [Fig. 1(c)]. In addition, the ELF attractor in the Hf_4 tetrahedron penetrates to the Hf_6 octahedron, with a finite value of ELF between two polyhedrons [Figs. 1(c) and 1(d)], suggesting the strong interaction between them, possibly due to the short distance (∼2.13 Å).

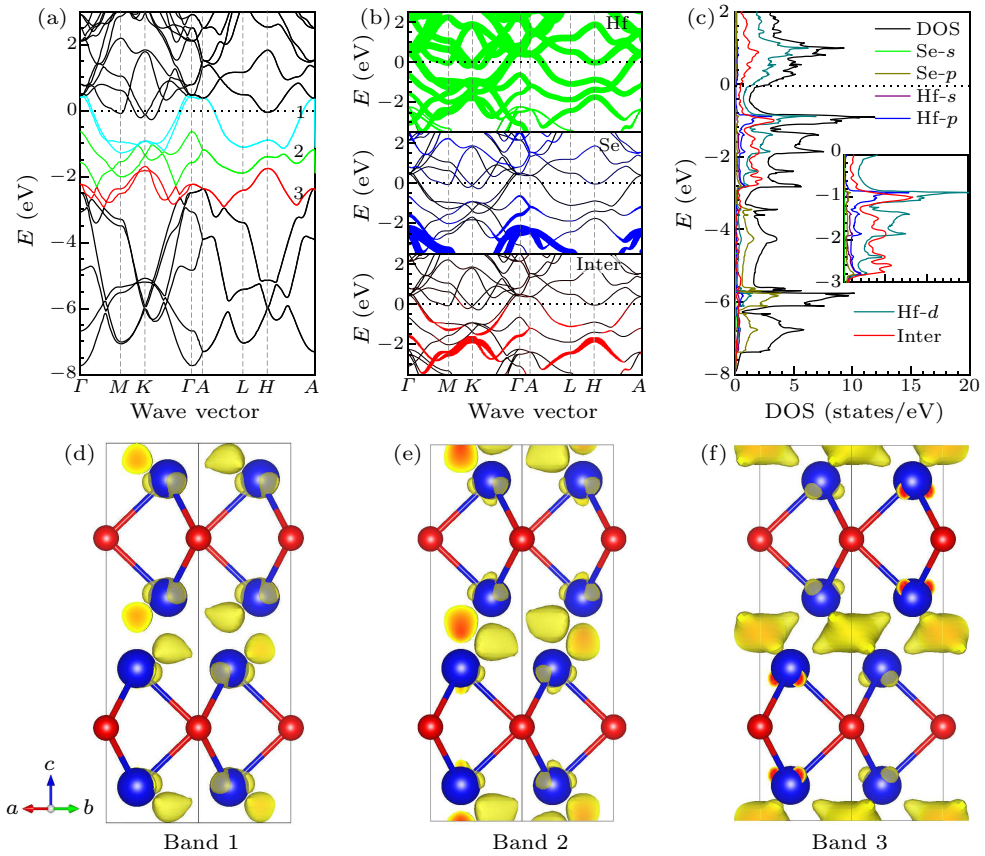

Fig. 2. (a) Total and (b) projected band structures of Hf_2Se. (c) Total and projected density of states (DOS) of Hf_2Se. The inset shows the enlarged part of the DOS in the energy range −3 eV to 0 eV. The Fermi level E_F is set to zero. (d), (e), and (f) The partial charge densities with an isosurface value of $1.3 \times 10^{-2} e/Å^3$ for band pairs 1, 2, and 3, respectively.

To further evaluate the electride characteristics of Hf_2Se, we investigated the band structure and the partial charge densities for bands near the Fermi level. Figure 2(a) shows the band structure of Hf_2Se, with six bands between −3.5 and 0 eV (E_F), denoted as band pairs 1, 2, and 3. It should be noted that there are two Hf_2Se formulae for one unit cell ($Z = 2$). In order to identify the contributions of interstitial electrons, the charge density was decomposed over the atom-centered spherical harmonics with a Wigner–Seitz radius of 1.56 Å, and the interstitial region was set as an empty sphere, placed at the center of the Hf_6 octahedral site.[9,33] The projected band structures and density of states (pDOS) in Figs. 2(b) and 2(c) show the contribution of Hf and Se elements to the bands in the vicinity of the Fermi surface. The existence of bands crossing the Fermi energy level E_F indicates that Hf_2Se may exhibit metallic behavior. The band structure and DOS of Hf_2Se are similar to those of Hf_2S.[24] From the pDOS, we learn that between −8 and −3.5 eV, the Se-2p states are dominant, with a minor contribution from Hf-3d states. This confirms the strong ionic bonding between Hf and Se atoms, which is consistent with the ELF analysis. The three band pairs near the Fermi surface are mainly derived from Hf-5d states and interstitial electrons [inset of Fig. 2(c)]. We observe that in the energy range of band pair 3, the contribution from the interstitial sites is comparable to the pDOS of Hf atoms. The significant pDOS contributed by the interstitial sites is a typical characteristic of electrides, similar to that observed with respect to Ca_2N and Y_2C.[9,10] The partial charge density (PCD) results further confirm the origin of the three band-pairs, as shown in Figs. 2(d)–

2(f). The PCD of band-pair 3 distributes dominantly in the Hf_6 octahedron, corresponding to the ELF attractor at site B [Fig. 1(d)]. Due to the full occupancy of band pair 3, there should be two anionic electrons per Hf_2Se formula, located at the Hf_6 octahedron. In contrast, in the energy ranges of band pairs 1 and 2, the pDOS of the Hf-5*d* state is larger than that of the interstitial electrons. The PCDs in Figs. 2(d) and 2(e) clearly indicate that these band pairs are mainly formed by the electrons in the Hf_4 tetrahedral sites. Moreover, these strongly localized electrons lead to the strong ELF attractor at site A [Fig. 1(c)]. Due to the (nearly) fully occupied band pair 2(1), there are approximate four electrons per Hf_2Se formula, situated at the Hf_4 tetrahedral sites. In addition, the energy overlap of these three band pairs indicates the strong interaction between the electrons in the Hf_4 tetrahedra and Hf_6 octahedra, which is in accord with the results of the ELF. Although the electrons in the voids of both Hf polyhedrons exhibit similar features, such as obvious ELF attractors, as well as large PCDs, it is likely that those electrons in site A may not be the anionic electrons, but may instead form Hf–Hf multiple-center metallic bonding states, since the Hf_4 tetrahedron has a relatively small volume V ($\sim$5.26 Å^3) with a much shorter distance, d_{cv}, between the center and the vertex of the tetrahedron ($\sim$2.13 Å) as compared to those of the Hf_6 octahedron (V = 21.12 Å^3, d_{cv} = 2.51 Å). A similar situation has been observed for YCl and Y_2Cl_3.[17] Based on the above analysis, the compound of Hf_2Se may be expressed as $[Hf_2Se]^{2+} \cdot 2e^-$. Taking into account that the anionic electrons in Hf_6 octahedra come primarily from the Hf-5*d* orbitals, the interstitial electrons in Hf_2Se thus originate from Hf-5*d* electrons, and coexist with the localized Hf–Hf metallic bonds, a process which differs from that of the well-known 2D electrides such as Ca_2N and Y_2C, whose anionic electrons come from the *s*-orbital electrons of Ca or Y atoms.

Given that interstitial electrons in electrides play the role of anions, in general, true anions could be inserted into the interstitial sites to host anionic electrons without introducing a large lattice strain.[8,17,34] More importantly, the inserted anions will significantly alter the band structure, particularly with respect to bands originating from the anionic electrons, and their related physical properties. For example, the substitution of chlorine atoms for anionic electrons leads to a transition from ferromagnetic $[Gd_2C]^{2+} \cdot 2e^-$ to antiferromagnetic Gd_2CCl by attenuating the interatomic exchange interactions.[34] Since the interstitial void of the Hf_6 octahedron in Hf_2Se should host two anionic electrons, here oxygen atoms are inserted into the centers of Hf_6 octahedra [denoted by small green balls in Fig. 3(a)] where the Wyckoff position of O atoms is (0, 0, 0). Figure 3(b) illustrates the ELF of Hf_2SeO with an isosurface value of 0.65. We observe nearly spherically distributed ELF attractors at the centers of the Hf_6 octahedra, indicating the ionic bonding between Hf and O atoms. This is similar to the case of Y_5Si_3H.[34] At the same time, it can be seen that the ELF attractors in the Hf_4 tetrahedra of Hf_2SeO shrink when compared to those of Hf_2Se [see Fig. 1(b)]. This suggests that the inserted O atoms have a significant influence on the electrons in the Hf_4 tetrahedra, due to strong Coulomb interaction between them at so short a distance. The band structure, total DOS, and pDOS of Hf_2SeO are shown in Fig. 3(c). Band pairs 1 and 2, mainly composed mainly of Hf-5*d* orbitals, are still between -3 and 0 eV (E_F), similar to Hf_2Se, but the dispersions of these bands change to some extent due to the presence of O atoms, which is consistent with the results of the ELF. In contrast, band pair 3, originating from the anionic electrons in Hf_2Se, disappears; instead, bands of oxygen 2*p* orbitals emerge in the range of -9 to -7 eV below the E_F. In this way, the anionic electrons in the Hf_6 octahedra have been completely transferred to O ions, and the formal valence state of Hf_2SeO should be $[Hf_2Se]^{2+}O^{2-}$. Such evolution of the band structure has also been observed in Y_5Si_3H and $NaBa_2OH$.[34,35] Briefly, the above results further suggest that the interstitial electrons at the Hf_6 octahedra of Hf_2Se are anionic.

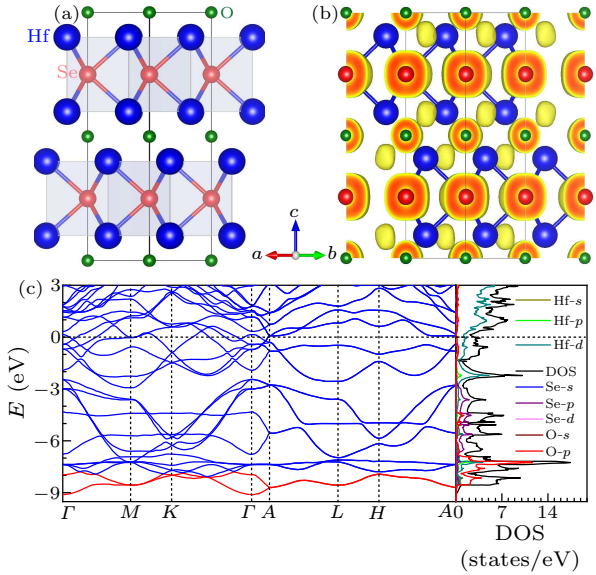

Fig. 3. (a) Crystalline structure of Hf_2SeO. The small green balls represent the O atoms located at the center of the Hf_6 octahedra. (b) ELF with an isosurface value of 0.65 for Hf_2SeO. (c) Band structure, total DOS and pDOS of Hf_2SeO. The Fermi level E_F is set to zero. Those bands consisting primarily of O-2*p* states are highlighted by red lines.

A low work function, possibly owing to the relatively loose anionic electrons, is another unique feature of electrides.[9,10,27] We therefore investigated the work function, Φ_{WF}, of Hf_2Se, using the slab models presented in Fig. 4. The calculated Φ_{WF} of the (110) and (001) surfaces of Hf_2Se are about 3.33 and

4.18 eV, respectively. The different work functions of these two surfaces indicate the obvious anisotropic characteristics of Hf_2Se. Both these values are rather low for an ionic compound,[36–40] and are comparable to those of Y_2C (3.08 eV),[10] revealing the electride nature of Hf_2Se with loosely bound electrons. The Φ_{WF} of the (110) surfaces is slightly smaller than that found in Hf_2S ($\Phi_{WF} \sim 3.6$ eV).[24] Since Hf_2S exhibits a self-passivated behavior with a strong oxidation resistance in water and acid solutions, resulting in an electrocatalytic reaction with excellent long-term sustainability,[24] it would be very interesting to verify whether Hf_2Se will also show comparable or even better electrocatalytic performance in the future.

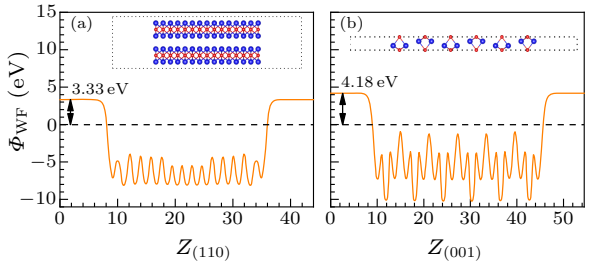

Fig. 4. Calculated work function of Hf_2Se for the (a) (110) and (b) (001) surfaces. Insets of (a) and (b) show the side views of the slab models for the (110) and (001) surfaces, respectively. The E_F is taken as zero (dashed line).

In summary, we have studied the electronic structures and the interesting features of the novel 2D electride candidate, Hf_2Se, based on first-principles calculations. Our results indicate that metallic Hf_2Se can host anionic electrons between $[Hf_2Se]$ layers, originating mainly from Hf-5*d* orbitals. These interstitial electrons coexist with Hf–Hf metallic bonds, such that the chemical formula of Hf_2Se could be written approximately as $[Hf_2Se]^{2+} \cdot 2e^-$. Moreover, Hf_2Se exhibits relatively low work functions. This study should shed light on discovering and designing novel electrides with multiple functions for practical applications.

References

[1] Dye J L 2009 *Acc. Chem. Res.* **42** 1564
[2] Dye J L 2003 *Science* **301** 607
[3] Kitano M, Inoue Y, Yamazaki Y, Hayashi F, Kanbara S, Matsuishi S, Yokoyama T, Kim S W, Hara M and Hosono H 2012 *Nat. Chem.* **4** 934
[4] Toda Y, Yanagi H, Ikenaga E, Kim J J, Kobata M, Ueda S, Kamiya T, Hirano M, Kobayashi K and Hosono H 2007 *Adv. Mater.* **19** 3564
[5] Ma Y, Eremets M, Oganov A R, Xie Y, Trojan I, Medvedev S, Lyakhov A O, Valle M and Prakapenka V 2009 *Nature* **458** 182
[6] Dong X, Oganov A R, Goncharov A F, Stavrou E, Lobanov S, Saleh G, Qian G R, Zhu Q, Gatti C, Deringer V L, Dronskowski R, Zhou X F, Prakapenka V B, Konôpková Z, Popov I A, Boldyrev A I and Wang H T 2017 *Nat. Chem.* **9** 440
[7] Matsuishi S, Toda Y, Miyakawa M, Hayashi K, Kamiya T, Hirano M, Tanaka I and Hosono H 2003 *Science* **301** 626
[8] Zhang Y, Xiao Z, Kamiya T and Hosono H 2015 *J. Phys. Chem. Lett.* **6** 4966
[9] Lee K, Kim S W, Toda Y, Matsuishi S and Hosono H 2013 *Nature* **494** 336
[10] Zhang X, Xiao Z, Lei H C, Toda Y, Matsuishi S, Kamiya T, Ueda S and Hosono H 2014 *Chem. Mater.* **26** 6638
[11] Inoshita T, Jeong S, Hamada N and Hosono H 2014 *Phys. Rev. X* **4** 031023
[12] Tsuji Y, Dasari P L, Elatresh S, Hoffmann R and Ashcroft N 2016 *J. Am. Chem. Soc.* **138** 14108
[13] Druffel D L, Kuntz K L, Woomer A H, Alcorn F M, Hu J, Donley C L and Warren S C 2016 *J. Am. Chem. Soc.* **138** 16089
[14] Zhao S, Li Z and Yang J 2014 *J. Am. Chem. Soc.* **136** 13313
[15] Inoshita T, Tsukada M, Saito S and Hosono H 2017 *Phys. Rev. B* **96** 245303
[16] Kim S, Song S, Park J, Yu H S, Cho S, Kim D, Baik J, Choe D H, Chang K J, Lee Y H, Kim S W and Yang H 2017 *Nano Lett.* **17** 3363
[17] Wan B, Lu Y, Xiao Z, Muraba Y, Kim J, Huang D, Wu L, Gou H, Zhang J, Gao F, Mao H K and Hosono H 2018 *npj Comput. Mater.* **4** 77
[18] Chanhom P, Fritz K E, Burton L A, Kloppenburg J, Filinchuk Y, Senyshyn A, Wang M, Feng Z, Insin N, Suntivich J and Hautier G 2019 *J. Am. Chem. Soc.* **141** 10595
[19] Burton L A, Ricci F, Chen W, Rignanese G M and Hautier G 2018 *Chem. Mater.* **30** 7521
[20] Tada T, Takemoto S, Matsuishi S and Hosono H 2014 *Inorg. Chem.* **53** 10347
[21] Ming W, Yoon M, Du M H, Lee K and Kim S W 2016 *J. Am. Chem. Soc.* **138** 15336
[22] Zhang Y, Wang H, Wang Y, Zhang L and Ma Y 2017 *Phys. Rev. X* **7** 011017
[23] Wang J, Hanzawa K, Hiramatsu H, Kim J, Umezawa N, Iwanaka K, Tada T and Hosono H 2017 *J. Am. Chem. Soc.* **139** 15668
[24] Kang S H, Bang J, Chung K, Nandadasa C N, Han G, Lee S, Lee K H, Lee K, Ma Y, Oh S H, Kim S G, Kim Y M and Kim S W 2020 *Sci. Adv.* **6** eaba7416
[25] Kresse G and Furthmüller J 1996 *Phys. Rev. B* **54** 11169
[26] Perdew J P, Burke K and Ernzerhof M 1996 *Phys. Rev. Lett.* **77** 3865
[27] Uijttewaal M A, Wijs G A and de Groot R A 2004 *J. Appl. Phys.* **96** 1751
[28] Franzen H F, Smeggil J G and Conard B R 1967 *Mater. Res. Bull.* **2** 1087
[29] Whittingham M S and Gamble F R 1975 *Mater. Res. Bull.* **10** 363
[30] Becke A D and Edgecombe K E 1990 *J. Chem. Phys.* **92** 5397
[31] Li Z, Yang J, Hou J G and Zhu Q 2004 *Angew. Chem. Int. Ed.* **43** 6479
[32] Savin A, Nesper R, Wengert S and Fässler T F 1997 *Angew. Chem. Int. Ed. Engl.* **36** 1808
[33] Miao M and Hoffmann R 2015 *J. Am. Chem. Soc.* **137** 3631
[34] Lu Y, Li J, Tada T, Toda Y, Ueda S, Yokoyama T, Masaaki K and Hosono H 2016 *J. Am. Chem. Soc.* **138** 3970
[35] Wang J, Zhu Q, Wang Z and Hosono H 2019 *Phys. Rev. B* **99** 064104
[36] Wang S, Chou J P, Ren C D, Tian H Y, Yu J, Sun C L, Xu Y J and Sun M L 2019 *Sci. Rep.* **9** 5208
[37] Wang H, Chen X, Xu G X and Huang K M 2015 *Chin. Phys. B* **24** 077305
[38] Wang H, Jiang L L, Lin P X, Lei S Q and Yu H Y 2018 *Chin. Phys. B* **27** 127302
[39] Li D Y, Sun L, Zhang S D, Wang Y, Liu X Y and Han R Q 2007 *Chin. Phys.* **16** 0240
[40] He Y, Zhang M, Zhang J Y, Wang Y and Yu Z P 2009 *Chin. Phys. Lett.* **26** 027302